Interaction of Phonons with Dislocations

Y. Kogure,[1,*] T. Kosugi,[1] and T. Nozaki[2]

[1]*Department of Physical Therapy, Teikyo University of Science and Technology, Uenohara, Yamanashi, Japan*

[2]*Department of Environmental Science, Teikyo University of Science and Technology, Uenohara, Yamanashi, Japan*

(Received April 12, 2010)

Motion of edge dislocations interacting with phonons has been simulated by means of a molecular dynamics method. The embeddedatom-method potential for copper is adopted in the simulation. Excitation of the dislocation atoms by the propagation of phonon (hot atom) is observed in the simulation. The motion of splitted dislocation under a shear stress is also investigated by highlighting the dislocation lines.

PACS numbers: 63.20 kp, 83.10 Rs

I. INTRODUCTION

The interaction of phonon with dislocation is deeply related to the thermal properties and mechanical properties of the materials. In general, the thermal conductivity of the crystalline solid shows a peak at low temperatures, and the influence of the phonon scattering by the dislocation is seen on the low-temperature side of the peak. The theoretical calculation of the thermal resistance by the dislocation was performed first by Klemens [1]. He treated the interaction of the phonon with dislocation based on elastic anharmonicity of a dislocation strain field. One of the present authors, Kogure, performed the detailed calculation that considered the anisotropy of the crystal [2]. Therefore, the third-order elastic constants measured by a ultrasonic experiments was used. On the other hand, Ninomiya developed a theory of the resonance scattering of the phonon by the dislocation based on the string model [3]. Northrop *et al.* investigated the dislocation-phonon interaction by using the heat pulse experiment [4]. In this paper, the dislocation-phonon interaction is studied by using the molecular dynamics (MD) computer simulation, where the embedded atom method potential developed by one of the author is adopted [5]. The potential function is successfully applied in the simulation of crystal defects and nanoparticles [6–9].

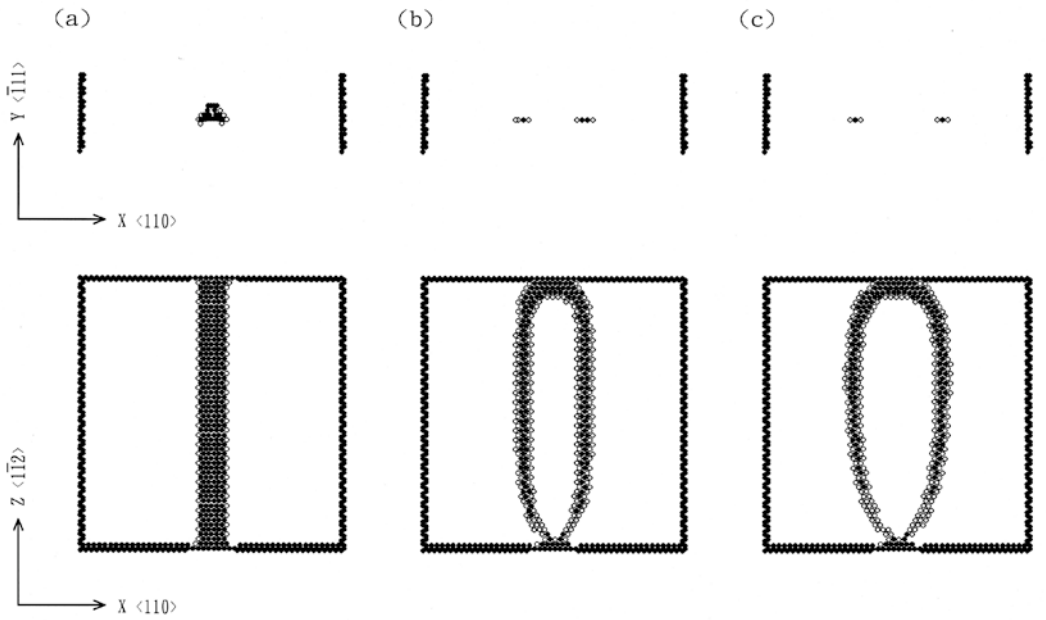

FIG. 1: Configuration of atoms around an edge dislocation (a) before, (b) in the middle of, and (c) after the initial relaxation under the fixed-boundary condition. A part of atomic plane perpendicular to the dislocation line is shown in the upper section, and an atomic plane parallel to the line is shown in the lower section. S represents MD time step. Open circles show atoms with the potential energy, -3.5 eV $< E < -3.485$ eV and solid circles express atoms $E \geq -3.485$ eV.

II. METHOD OF SIMULATION

Molecular dynamics simulation has been performed by using an embedded atom method potential. The potential energy for the i–th atom is expressed as

$$E_i = F(\rho_i) + \sum_j \phi(r_{ij})/2, \tag{1}$$

where $F(\rho_i)$ is the embedding energy for the i–th atom and ρ_i is the electron density function, which is a sum of electron density of neighbor atom labeled by j. These are expressed as

$$F(\rho_i) = D\rho_i \ln \rho_i, \tag{2}$$

$$\rho_i = \sum_j f(r_{ij}), \tag{3}$$

and $\phi(r_{ij})$ is the two-body interaction between the atoms i and j. The functional form of $\phi(r)$ and $f(r)$ are

$$\phi(r) = A(r_{c1} - r)^2 \exp(-c_1 r), \tag{4}$$

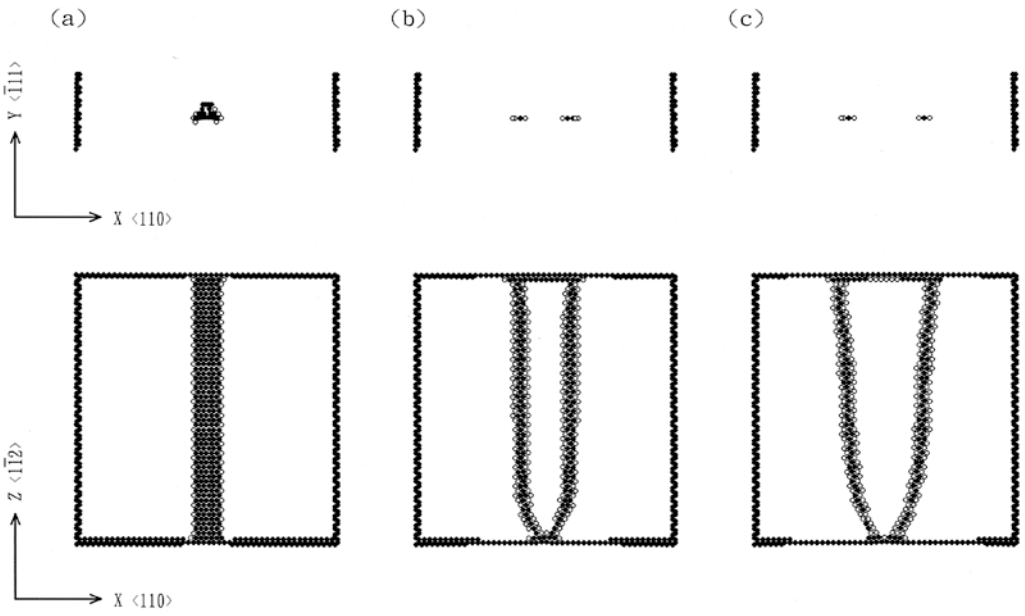

FIG. 2: Configuration of atoms around an edge dislocation (a) before, (b) in the middle of, and (c) after the initial relaxation under the free-boundary condition. The indication is the same as that of figure 1.

$$f(r) = B(r_{c2} - r)^2 \exp(-c_2 r), \tag{5}$$

where $r_{c1} = 1.6r_0$ and $r_{c2} = 1.9r_0$ are the truncation distance of the potential, and r_0 is the nearest neighbor distance. The potential parameters, A, B, D, c_1, c_2, for Cu are determined to reproduce the material properties such as the cohesive energy, the elastic constants, the vacancy formation energy and the stacking fault energy [5].

The time interval Δt for the simulation is chosen to be 1×10^{-15} s, which is less than 1/100 of the period of maximum atomic vibration frequency. The model crystal is covered by the $\{110\}, \{111\}$, and $\{112\}$ faces and consists of 143,000 atoms. Sizes are about $12 \times 10 \times 10$ nm in the x, y, z directions, respectively. Fixed- and free-boundary conditions are adopted, namely, atoms on the surfaces perpendicular to the dislocation line are fixed or released free. The dislocation is pinned down at the surfaces in the former. On the contrary, the dislocation can move freely in the latter. Atoms on the surfaces parallel to the dislocation line are fixed in both cases during simulation. Initially, a couple of extra $\{110\}$ atomic planes are inserted in the lower middle of the crystal to introduce an edge dislocation because the fcc crystal is constituted by two independent planes in the [110] direction, and the crystal is relaxed. The introduced dislocation is split into two partial dislocations as expected.

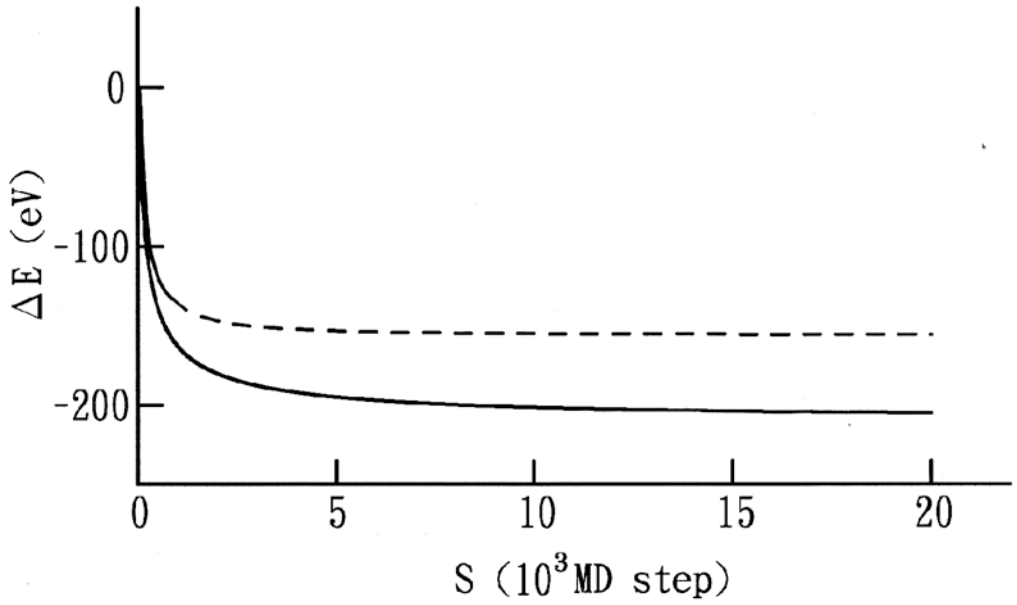

FIG. 3: Change in the total potential energy thorough initial relaxation. Solid line shows the result for fixed-boundary condition, and dashed line is for free-boundary condition.

III. RESULTS AND DISCUSSION

III-1. Initial Configuration

Initially, an edge dislocation is introduced. Configuration of atoms is shown in figure 1 (a), where atoms are displaced by the strain field given by the elasticity theory. The potential energy of each atom is calculated by equation (1); the atoms with potential energy larger than -3.5 eV are shown and atoms with higher potential energy $E \geq -3.485$ eV are highlighted by solid circles. Then, the molecular dynamics simulation was performed and the crystal was relaxed. Result is shown in figure 1(c). Introduced dislocation is seen to be split into partial dislocations. A stacking fault structure is seen between two partial dislocations. Width of the stacking fault is known to be determined by the balance of the stacking fault energy and the repulsive force between two partial dislocations; but, the effect of fixed boundary may reduce the width of stacking fault. Vertical view of atomic planes is shown in the upper section of each figure. It is seen that the split dislocation is confined in an atomic plane after the initial relaxation.

Results for the relaxation under the free-boundary condition are shown in figure 2. It is seen that the splitting of the dislocation becomes larger toward the top. This asymmetric configuration in the z-direction may be due to the crystal structure. It is noted that six distincttypes of atomic planes are stacked upon one another in a repeating sequence as ABCDEFABCDEF... in the [112] direction, and it is not symmetric in the top and bottom

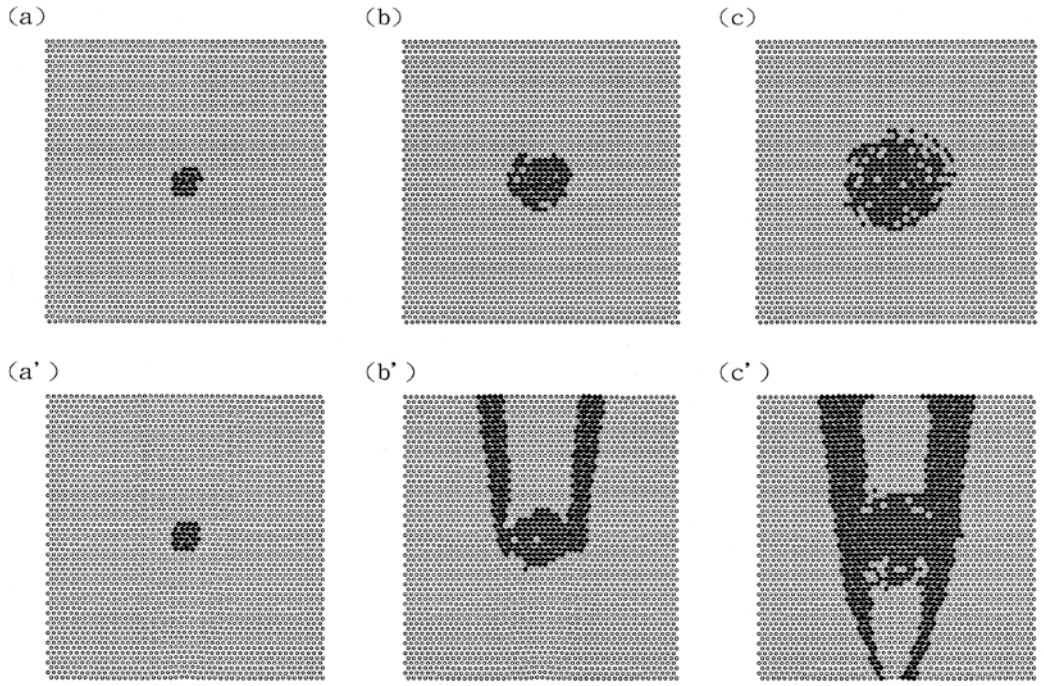

FIG. 4: Evolution of hot atoms at (a) 50 MD step, (b) 250 MD step, and (c) 750 MD step in a perfect crystal. Solid circles show hot atoms. Figures (a′), (b′) and (c′) show the evolution at same MD steps in a crystal with dislocation.

directions. On the other hand, the dislocation is fixed on the upper and lower boundary for the fixed-boundary condition as shown in figure 1. However, the shape of the split dislocation between the two boundaries is seen to be asymmetric, and the width of the split tends to be larger toward the upper direction. A study based on crystallography will be made in the future.

The change in the total potential energy, $\Delta E = \sum_i E_i - \sum_i E_{0i}$, is shown in figure 3, where E_{0i} is the potential energy for i–th atom at the initial condition. ΔE is larger for the free-boundary condition than for fixed-boundary condition, which reaches about 200 eV. The value of the relaxed energy for the free-boundary condition per unit dislocation length (0.24 nm) can be estimated to be 2.4 eV, which is smaller than the cohesive energy and larger than the vacancy-formation energy of copper.

III-2. Propagation of hot atom

An initial velocity with random magnitude and direction is given to the atoms near the center of model crystals, and the development of the atomic velocity is monitored. Here, 'hot atom' is defined as an atom, which has larger velocity (vibration energy) than environmental atoms. Simulations were performed for two samples with the same size.

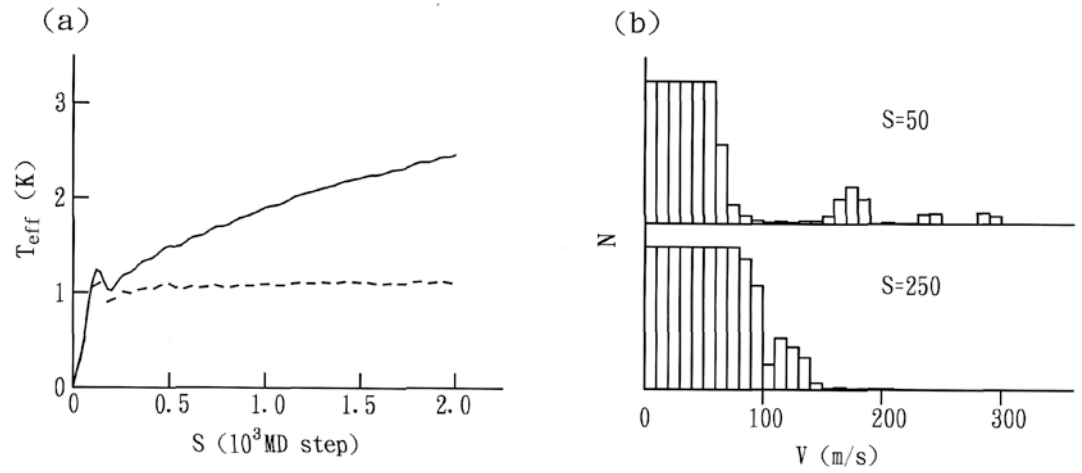

FIG. 5: Variation in the effective temperature in the crystal in which hot atoms are injected. The dashed line shows the result for a perfect crystal and the solid line is for a crystal with dislocation (a). Histograms of velocity distribution at typical time steps (b).

One was the perfect crystal and the other contained split partials. Distributions of hot atoms at typical time step in both samples are compared in figure 4, in which the hot atoms are shown by solid circles. A region occupied by hot atoms develops spherically and diffusively in the perfect crystal. On the contrary hot atom region develops non-uniformly in the crystal with dislocation. When the border of hot region reaches the position of the partial dislocations, many atoms constituting the dislocation are exited and become hot atoms. Atoms on the dislocation line are unstable and mobile, and they start to move by the excitations. The phenomenon may be described as the absorption of phonons by some localized dislocation modes. The total kinetic energy of atoms in the crystals is expressed by the effective temperature T_{eff}, which is calculated from the kinetic energy of atoms [10]. Variations of the effective temperature with MD steps in both samples are shown in figure 5(a), and the histograms for the velocity distribution in the crystal with dislocation are shown in figure 5(b). It is seen that the system is not in thermal equilibrium at early stage of the MD step. As the MD time step proceeds, the velocity distribution moves to the low-value side, and the number of atoms with large velocity decreases. On the other hand, region exited by hot atoms expands diffusively. The effective temperature increases to about 1 K by injection of hot atoms, and it is mostly constant in the perfect crystal, whereas the temperature gradually increases in the crystal with dislocation. The increased energy may be due to the structural relaxation of dislocation.

III-3. Motion of dislocation under a stress

Shear strain $\varepsilon_{xy} = 0.05$ to move the dislocation in the $-x$ direction was applied as a step function of time, and the system was relaxed under the fixed-boundary condition. Then the motion of dislocation was monitored. The initial temperature was set to be 0 K,

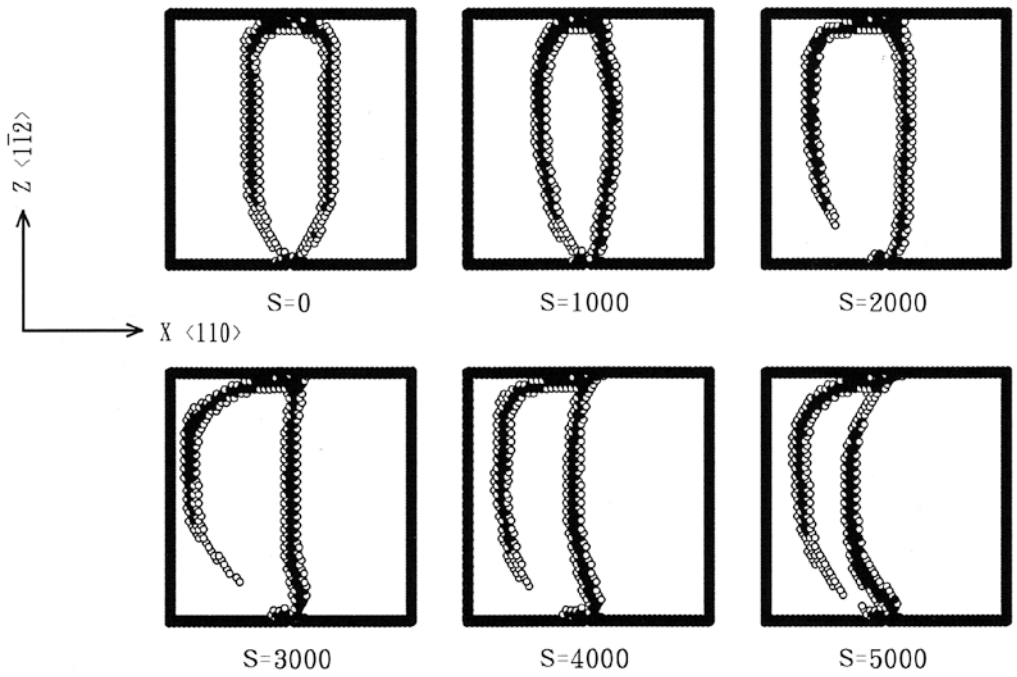

FIG. 6: Motion of split edge dislocation under a fixed-boundary condition. S represents MD time steps. The indication for atoms is the same as that in figure 1.

but it was slightly increased up to 6 K with the molecular dynamics (MD) time steps. Snap shots of the dislocation configuration at typical MD time steps are shown in figure 6, where only atoms with higher potential energy $E > -3.5$ eV are shown, and the atoms with the potential energy higher than -3.485 eV are marked by solid circles. These open and solid circles characterize the internal structure of the dislocations. In figure 6, the dislocations are pinned at the top and bottom surfaces by adopting the fixed-boundary condition. Initially, one of the partial dislocation moves toward the left direction ($S = 2000$), then another one follows. Both dislocations form bow shape as a balance of external stress and line tension of dislocations. Afterward, it was pushed back by the mirror force due to the fixed boundary. These motions are repeated. The period of the dislocation oscillation is about 100 times that of the thermal lattice vibration.

Similar simulation under the free-boundary condition was also performed, and the results are shown in figure 7. The shapes of the dislocations are very wavy and many kinks seem to be present on the Peierls hills, which run along the vertical direction on a slip plane. As the dislocations are widely spread on a [111] plane, they are always confined in an atomic plane, namely, climbing is not observed in the simulation.

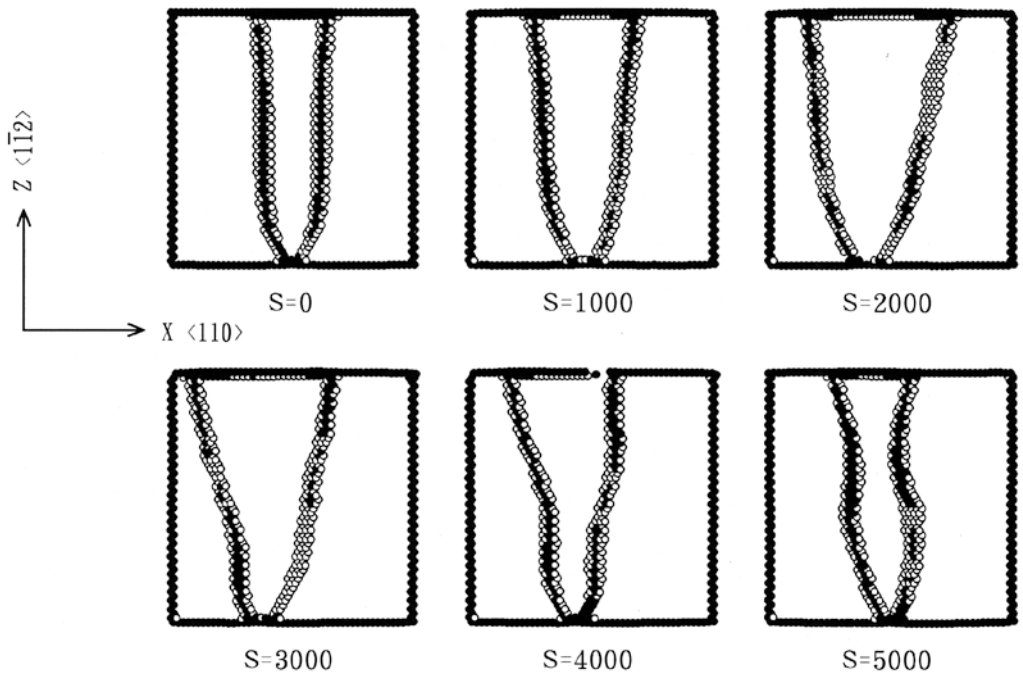

FIG. 7: Motion of split edge dislocation under a fixed-boundary condition. S represents MD time steps. The indication for atoms is the same as that in figure 1.

The mean shear strain ε_m in the crystal is calculated by the relation,

$$\varepsilon_m = \frac{1}{N}\sum_{i=1}^{N}\frac{x_i - x_{0i}}{y_{0i}} \tag{6}$$

Here, x_{0i} and y_{0i} are x, y coordinates of the i–atom at initial state. The calculated results for the fixed- and the free-boundary conditions are shown in figure 8(a). The strain is seen to increase once and then to decrease during a simulation under the fixed-boundary condition. The strain is seen to increase one-sidedly under the free-boundary condition. The mean temperature is also calculated, and the results are shown in figure 8(b). The mean temperature increased largely under the free-boundary condition, whereas the temperature change was very small under the fixed-boundary condition. Large energy dissipation seems to be happened in the sample under the free-boundary condition.

IV. CONCLUSIONS

EAM potential has successfully been applied on the molecular dynamics simulation of moving dislocations in a copper crystal. Both fixed- and free-boundary conditions were

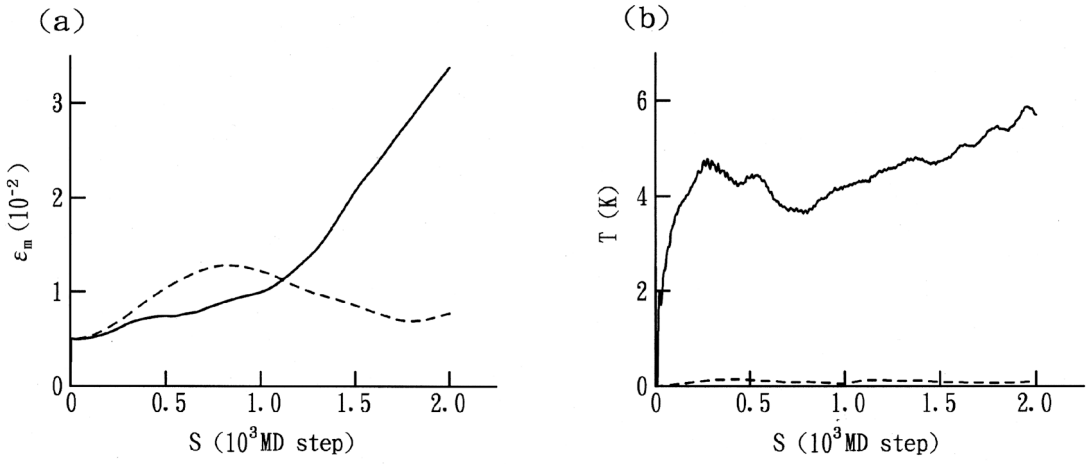

FIG. 8: (a) Change in mean strain ε_m and (b) mean temperature $\overline{T}$ in the crystal with moving dislocation. The solid lines show the results for the free-boundary condition and the dashed line shows the results for fixed boundary.

adopted, and the results were compared. A dislocation was split into partials and a stacking fault appeared between the partials. The configuration of dislocations was displayed by highlighting the atoms with larger potential energy. Hot atoms were injected at the center of crystal, and the propagation of hot atoms was investigated. The atoms constituting dislocation were highly excited by the hot atoms. The motion of split partial dislocations under a shear stress was simulated. Wavy motion of partial dislocations on a {111} plane was observed under the fixed- and free-boundary conditions.

References

* Electronic address: kogure@ntu.ac.jp

[1] P. G. Klemens, Proc. Phys. Soc. A **68**, 1113 (1955).
[2] Y. Kogure and Y. Hiki, J. Phys. Soc. Jpn. **38**, 471 (1975).
[3] T. Ninomiya, J. Phys. Soc. Jpn. **25**, 830 (1968).
[4] G. A. Northrop, E. J. Cotts, A. C. Anderson and J. P. Wolfe, Phys. Rev. Lett. **49**, 54 (1982).
[5] M. Doyama and Y. Kogure, Radiat. Effects Defects Solids **142**, 107–114 (1997).
[6] Y. Kogure, J. Alloys Comp. **355**, 188–195 (2002).
[7] Y. Kogure, T. Kosugi and M. Doyama, Mater. Sci. Eng. A **370**, 100–104 (2004).
[8] Y. Kogure, T. Kosugi, M. Doyama and H. Kaburaki, Mater. Sci. Eng. A **442**, 71–74 (2006).
[9] Y. Kogure, T. Kosugi, T. Nozaki and M. Doyama, Mater. Sci. Eng. A **521–522**, 30–33 (2009).
[10] D. G. Cahill, W. K. Ford, K. E. Goodson, G. D. Mahan, A. Majumdar, H. J. Maris, R. Merlin and S. R. Phillpot, J. Appl. Phys. **93**, 793–818 (2003).